Divergent Roles for Maize PAN1 and PAN2 Receptor-Like Proteins in Cytokinesis and Cell Morphogenesis[1][W][OPEN]

Dena Sutimantanapi, Dianne Pater, and Laurie G. Smith*

Section of Cell and Developmental Biology, University of California San Diego, La Jolla, California 92093–0116

ORCID ID: 0000-0002-8294-1589 (L.G.S.).

Pangloss1 (PAN1) and PAN2 are leucine-rich repeat receptor-like proteins that function cooperatively to polarize the divisions of subsidiary mother cells (SMCs) during stomatal development in maize (*Zea mays*). PANs colocalize in SMCs, and both PAN1 and PAN2 promote polarization of the actin cytoskeleton and nuclei in these cells. Here, we show that PAN1 and PAN2 have additional functions that are unequal or divergent. PAN1, but not PAN2, is localized to cell plates in all classes of dividing cells examined. *pan1* mutants exhibited no defects in cell plate formation or in the recruitment or removal of a variety of cell plate components; thus, they did not demonstrate a function for PAN1 in cytokinesis. PAN2, in turn, plays a greater role than PAN1 in directing patterns of postmitotic cell expansion that determine the shapes of mature stomatal subsidiary cells and interstomatal cells. Localization studies indicate that PAN2 impacts subsidiary cell shape indirectly by stimulating localized cortical actin accumulation and polarized growth in interstomatal cells. Localization of PAN1, Rho of Plants2, and PIN1a suggests that PAN2-dependent cell shape changes do not involve any of these proteins, indicating that PAN2 function is linked to actin polymerization by a different mechanism in interstomatal cells compared with SMCs. Together, these results demonstrate that PAN1 and PAN2 are not dedicated to SMC polarization but instead play broader roles in plant development. We speculate that PANs may function in all contexts to regulate polarized membrane trafficking either directly or indirectly via their influence on actin polymerization.

Leucine-rich repeat (LRR)-receptor-like kinases (RLKs) regulate many aspects of plant development and physiology. While few ligands have been definitively identified, the general view of the function of these proteins is that interaction of ligand(s) with the LRR-containing extracellular domains regulates the activity of the intracellular kinase domains, triggering downstream cellular responses. While the kinase domains of many such receptor-like proteins appear to be catalytically inactive (an estimated approximately 20% of all Arabidopsis [*Arabidopsis thaliana*] RLKs, based on bioinformatics analyses; Castells and Casacuberta, 2007), many such "pseudokinases" nevertheless participate in signal transduction via interaction with active kinases (other LRR-RLKs or cytoplasmic kinases; Llompart et al., 2003; Boudeau et al., 2006; Rajakulendran and Sicheri, 2010).

We previously identified a pair of LRR-RLKs in maize (*Zea mays*), Pangloss1 (PAN1) and PAN2, which function cooperatively to polarize the asymmetric divisions of subsidiary mother cells (SMCs) during stomatal development (Cartwright et al., 2009; Zhang et al., 2012). In response to hypothetical polarizing cues from the adjacent guard mother cell (GMC), premitotic SMCs polarize toward the GMC, involving migration of the nucleus to the site of GMC contact and the formation of a pronounced enrichment of cortical F-actin at that site. Subsequently, SMCs divide asymmetrically to produce subsidiary cells flanking the GMC, which in turn divides to produce a guard cell pair (Galatis and Apostolakos, 2004). In *pan1* and *pan2* mutants, defects in premitotic SMC polarization (evident from a lack of nuclear polarization and/or actin accumulation at the GMC contact site) lead to abnormally oriented divisions producing aberrantly shaped subsidiaries that often fail to differentiate correctly (Gallagher and Smith, 2000; Cartwright et al., 2009; Zhang et al., 2012). A function for PAN1 and PAN2 in responding to ligands produced by adjacent GMCs is consistent with the finding that both proteins accumulate in SMCs preferentially at the site of contact with GMCs, prior to actin accumulation and nuclear polarization to this site (Cartwright et al., 2009; Zhang et al., 2012). However, no ligands for PAN1 or PAN2 have yet been identified. A synergistic increase in the frequency of SMC polarity defects in *pan1;pan2* double mutants provides evidence of cooperative or partially redundant functions for these LRR-RLKs, but we found no evidence that they physically interact as expected for a coreceptor pair (Zhang et al., 2012). Instead, localization studies revealed that these proteins act sequentially, with PAN2 functioning upstream of PAN1, because the polarized accumulation of PAN1 at GMC contact sites of SMCs requires PAN2 but not vice versa (Cartwright et al., 2009; Zhang et al., 2012). The kinase domains of both PAN1 and PAN2 are inactive in vitro, as predicted from the lack of certain amino acids needed

[1] This work was supported by the National Science Foundation (grant no. IOS–1147265) and by the University of California Academic Senate (research grant to L.G.S.).

* Address correspondence to lgsmith@ucsd.edu.

The author responsible for distribution of materials integral to the findings presented in this article in accordance with the policy described in the Instructions for Authors (www.plantphysiol.org) is: Laurie G. Smith (lgsmith@ucsd.edu).

[W] The online version of this article contains Web-only data.

[OPEN] Articles can be viewed online without a subscription.

www.plantphysiol.org/cgi/doi/10.1104/pp.113.232660

for catalytic activity (Cartwright et al., 2009; Zhang et al., 2012), but both may function in signaling via a kinase domain-mediated association with active kinases. The downstream events linking PAN function to premitotic SMC polarization are largely unknown, but PAN1 functions cooperatively with, and physically interacts with, type I Rho of Plants (ROP) GTPases to promote SMC polarization (Humphries et al., 2011). Considering that Rho family GTPases including ROPs in plants are well known for their roles in regulating actin polymerization (Yalovsky et al., 2008), this finding suggests that ROPs link PAN1 to localized actin polymerization at GMC contact sites. However, the functional significance of localized actin accumulation at the GMC contact site of SMCs is unclear.

In addition to their function in maize SMC polarization, type I ROPs function in a variety of plant cells undergoing polarized cell expansion to mediate the localized accumulation of F-actin associated with localized expansion of the cell surface (Yalovsky et al., 2008). The roles of actin and ROPs in polarized cell growth have been studied in the context of tip-growing pollen tubes and root hairs as well as in epidermal pavement cells, where nonuniform patterns of cell expansion underlie the formation of lobes that interlock adjacent cells together. Arabidopsis ROP2 is enriched at sites of pavement cell lobe outgrowth, where it acts via the novel ROP effector ROP-Interactive CRIB Domain-Containing4 (RIC4) to stimulate localized cortical F-actin enrichment (Fu et al., 2005). Studies of the role of auxin and the auxin-binding protein ABP1 in this process support a model in which ABP1-auxin interaction at the cell surface signals through ROP2 and RIC4 to promote actin-dependent localized accumulation of the auxin efflux carrier PIN1, further increasing the local concentration of auxin and establishing a local feedback loop that promotes localized cell expansion (Xu et al., 2010; Yang and Lavagi, 2012). In pollen tubes, actin filaments provide both long- and short-range guidance for vesicles trafficking to and from the growth site and may also directly influence vesicle fusion and/or removal from the plasma membrane (Qin and Yang, 2011; Chebli et al., 2013). Thus, actin regulation of membrane trafficking plays a central role in polarized cell growth in all cell types where it has been studied, although the mechanisms by which actin influences these processes may not be the same in all cell types.

The cytoskeleton and membrane trafficking also play critical roles in plant cytokinesis. During somatic cell divisions, an actin- and microtubule-based structure called the phragmoplast forms between daughter nuclei after mitosis and functions as a dynamic scaffold for the assembly of a new cell wall (cell plate) separating the daughter cells (Jürgens, 2005). The cell plate is initiated via vesicle fusion at the phragmoplast equator and proceeds through a complex series of membrane-remodeling events to form a network of interconnected tubules and eventually a continuous sheet perforated by plasmodesmata, involving ongoing fusion and fission of vesicles (Samuels et al., 1995; Seguí-Simarro et al., 2004). A wide variety of proteins regulating vesicle targeting, fusion, and fission are localized to cell plate membranes, with variations in timing suggesting participation in distinct phases of cell plate formation (McMichael and Bednarek, 2013). The cell plate is also an active site of cell wall and membrane biosynthesis directed by enzymes that are recruited to the plate with characteristic timing (McMichael and Bednarek, 2013). Studies with cytoskeleton-disrupting drugs have clearly demonstrated an essential role for phragmoplast microtubules in transporting vesicles to the cell plate, but the role of phragmoplast F-actin is less clear (Jürgens, 2005). The mechanisms responsible for the coordination and temporal regulation of the complex events underlying cell plate formation during cytokinesis are largely unknown.

Here, we report new and unequal roles for PAN1 and PAN2 outside of SMCs. PAN1, but not PAN2, is localized to cell plates, although no essential function for PAN1 in cell plate formation was found via an analysis of *pan* mutants. PAN2 plays a greater role than PAN1 in the coordinated morphogenesis of interstomatal cells and stomatal subsidiary cells that produce the characteristic shapes of maize stomata. Thus, PANs do not always function cooperatively and have other roles besides the promotion of premitotic SMC polarization, with implications regarding the cellular processes in which these receptor-like proteins function.

RESULTS

PAN1 Is Recruited to Cell Plates in a PAN2-Independent Manner

PAN1 localization studies showed that in SMCs undergoing cytokinesis, PAN1 is enriched at cell plates as well as at the site of contact with the adjacent GMC. This was observed via live-cell imaging of native promoter-driven PAN1-yellow fluorescent protein (YFP; described by Humphries et al., 2011) in combination with cyan fluorescent protein (CFP)-tubulin to visualize phragmoplasts (Fig. 1A) and also via immunolocalization with a PAN1-specific antibody (Cartwright et al., 2009) with phalloidin counterstaining of phragmoplast F-actin (Fig. 1B). PAN1 is present at the earliest stage of cell plate formation in SMCs (Figure 1, arrowhead 1 in A and arrowhead in B), becoming more enriched at the cell plate later in areas where the phragmoplast has already disassembled and as the cell plate is attaching to the mother cell wall (Fig. 1A, arrowheads 2 and 3). Shortly after completion of the new subsidiary cell wall, PAN1 returns to levels similar to those seen at the mother cell periphery (Fig. 1A, arrowhead 4). Notably, PAN1 enrichment in cell plates is not unique to SMCs, as it is also observed in symmetrically dividing leaf epidermal cells; however, in these cells, it appears equally enriched at all stages of cell plate formation (Fig. 1, C–E). PAN1 is also enriched in cell plates of root cortical cells (Supplemental Fig. S1). Together, these observations suggest a function for PAN1 in cell plate formation in all cell types. This finding is consistent with the observation that PAN1 is expressed in a wide variety of tissues where

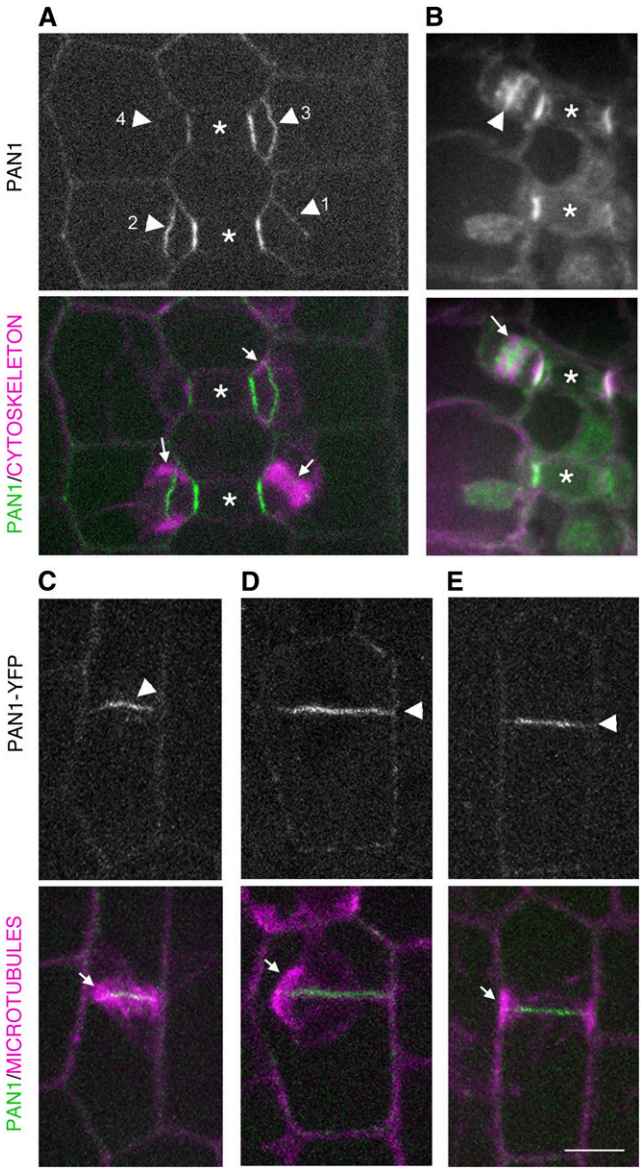

Figure 1. PAN1 is enriched at cell plates. A, PAN1-YFP shown in monochrome (top) and green (bottom). Asterisks mark GMCs. Arrowheads 1 to 4 point to SMC cell plates at successive stages, as indicated by the associated phragmoplast (magenta and marked with arrows at bottom). PAN1-YFP is enriched relative to mother cell walls in plates 2 and 3. B, Immunolocalization of endogenous PAN1 shown in monochrome (top) and green (bottom), with actin labeling via phalloidin staining shown in magenta at bottom. Asterisks mark GMCs. PAN1 staining of an SMC cell plate is marked by the arrowhead (top), with the associated phragmoplast marked by the arrow at bottom. Staining of the phragmoplast itself does not exceed the background observed when *pan1* protein null mutants are labeled in parallel. C to E, PAN1-YFP localization (monochrome at top and green at bottom) in three separate cells illustrating successive stages of cell plate formation, as indicated by the associated phragmoplasts (magenta) in transversely dividing epidermal cells. Arrowheads at top mark cell plates; arrows at bottom mark phragmoplasts. PAN1-YFP is enriched at cell plates relative to the surrounding mother cell surface to an approximately equal degree at all stages of cell plate development shown. Bar = 10 μm for all images.

cells are actively dividing, including embryos, ear and tassel primordia, and seedling primary roots (Cartwright et al., 2009; Sekhon et al., 2011).

PAN1 and PAN2 colocalize in premitotic SMCs at the site of GMC contact, and PAN2 is required for the accumulation of PAN1 at this site (Cartwright et al., 2009; Zhang et al., 2012). However, immunolocalization with anti-PAN2 and imaging of native promoter-driven PAN2-YFP (both described previously by Zhang et al., 2012) revealed no detectable localization of PAN2 at cell plates at any stage of SMC cytokinesis (Fig. 2, A–F). Consistent with this finding, PAN2 is not required for PAN1-YFP accumulation at cell plates (Fig. 2, G–J). Thus, PAN1 is recruited to cell plates by a PAN2-independent mechanism.

PAN1 Is Not Required for Cell Plate Formation

The observation that PAN1 is enriched at cell plates led us to ask whether there are defects in cell plate formation in SMCs or other cells in *pan* mutants. Although SMC walls are often misoriented in *pan1* and *pan2* single mutants, and considerably more so in *pan1;pan2* double mutants (Cartwright et al., 2009; Zhang et al., 2012), analysis of epidermal cell walls and nuclei visualized by acriflavine or propidium iodide staining of fixed tissues revealed no incomplete or missing cell walls in stomatal subsidiaries or other epidermal cells in any of these mutants ($n > 800$ cells per genotype). Since PAN1 function in premitotic SMCs promotes localized actin polymerization associated with polarization, we reasoned that PAN1 could similarly function at the cell plate surface to promote the polymerization of actin filaments in the phragmoplast. As illustrated in Supplemental Figure S2, F-actin was visualized in wild-type and *pan* mutant SMCs undergoing cytokinesis via phalloidin staining, but no difference was observed in the organization or density of F-actin in SMC phragmoplasts whether oriented normally (Supplemental Fig. S2B) or abnormally (Supplemental Fig. S2C; $n = 26$ wild-type and 31 *pan* mutant phragmoplasts examined).

To further investigate possible functions for PAN1 in cell plate formation, we tested whether the recruitment of a variety of other cell plate-localized molecules might be altered. The majority of research on cell plate formation has been carried out using Arabidopsis, and there is a paucity of previously characterized tools for the visualization of cell plate components in maize. Thus, we obtained antibodies raised against cell plate-localized proteins from other plants for which a maize homolog is identifiable in the genome, and the portion used for antibody production is well conserved in the maize homolog. Results are presented for four such antibodies that recognized maize proteins on immunoblots consistent with the predicted size of maize homologs (Supplemental Fig. S3) and labeled cell plates with some specificity via immunolocalization (Fig. 3), suggesting that these antibodies indeed recognize homologous proteins in maize. To facilitate analysis of the

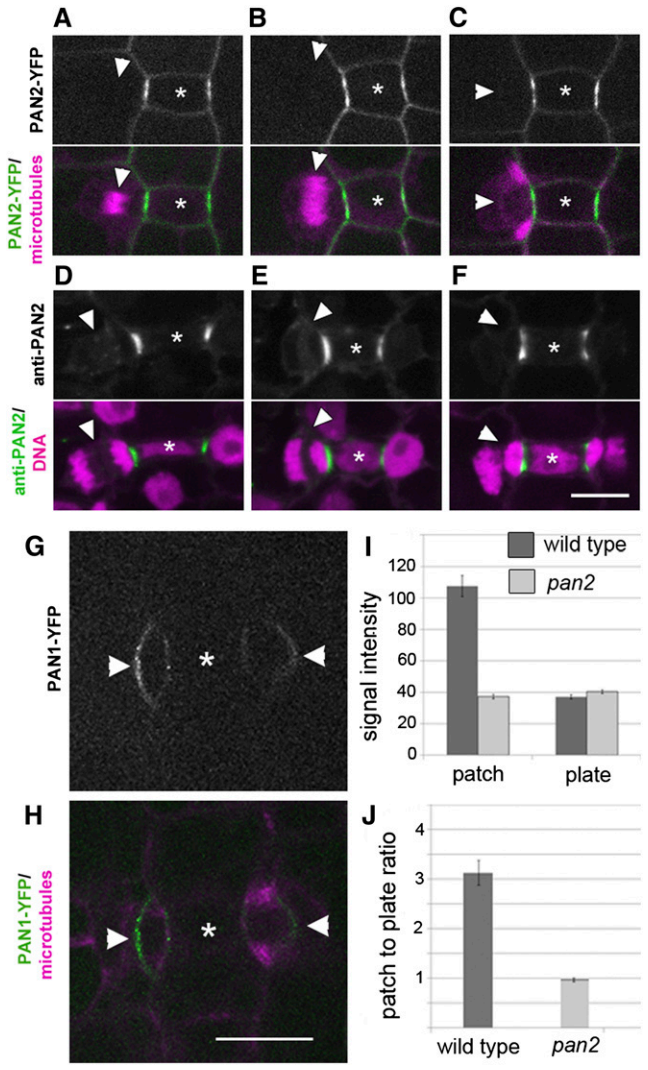

Figure 2. PAN2 is undetectable at cell plates and not required for cell plate localization of PAN1. A to C, PAN2-YFP shown in monochrome (top) and green (bottom), along with CFP-tubulin in magenta, at successive stages of cell plate formation seen in three separate SMCs. Asterisks mark GMCs, which are flanked by PAN2-YFP patches in adjacent SMCs. Arrowheads point to the locations of cell plates (with no detectable PAN2-YFP), as indicated by the positions of the associated phragmoplasts seen at bottom. D to F, Anti-PAN2 staining shown in monochrome (top) and green (bottom), along with propidium iodide-stained nuclei shown in magenta, at successive stages of cytokinesis seen in three separate SMCs. Asterisks mark GMCs, which are flanked by PAN2 patches in adjacent SMCs. Arrowheads point to the locations of cell plates (with no detectable PAN2 staining), as indicated by the positions of associated nuclei. Bar = 10 μm for A to F. G and H, PAN1-YFP (monochrome in A and green in B) in two *pan2-2* mutant SMCs flanking GMCs (asterisks), with arrowheads pointing to cell plates. As indicated by the presence of a late-stage phragmoplast (CFP-tubulin signal; magenta in H), the SMC on the right is nearing the point of cell plate attachment while the SMC on the left has a recently attached cell plate. Although these SMCs lack PAN1-YFP patches of normal intensity at the site of GMC contact (e.g. as seen for the wild type in Fig. 1), the PAN1-YFP signal level at cell plates is similar to that of the wild type. Bar = 10 μm. I, Quantitative analysis of PAN1-YFP signal intensity (arbitrary units as measured via ImageJ) in SMCs at GMC contact sites (patch) and the cell plate (plate). J, As in I, but with results shown as a ratio of signal measured at GMC contact sites versus the cell plate. n = 62 cells analyzed for the wild type and 72 cells analyzed for *pan2* mutants; error bars show SE. In wild-type SMCs, PAN1-YFP signal is approximately 3-fold stronger at GMC contact sites than at cell plates (patch-to-plate ratio of approximately 3). In *pan2* mutant SMCs, PAN1-YFP signal intensity is reduced at GMC contact sites but not at cell plates, reducing the patch-to-plate signal ratio to approximately 1.

timing of the recruitment and removal of each cell plate component, we divided SMC cytokinesis into five stages (illustrated in Fig. 3A), with cell plate attachment occurring between stage i and stage ii and subsequent stages distinguished according to the position and degree of decondensation of the daughter nuclei.

KNOLLE is a cell plate-specific syntaxin that mediates the fusion of cell plate vesicles (Lukowitz et al., 1996; Lauber et al., 1997). ADP Ribosylation Factor1 (ARF1) is a small GTPase that regulates the formation of vesicles at the Golgi and cell plate surface (Couchy et al., 2003), and Secretory Carrier Membrane Proteins (SCAMPs) are cell plate-localized proteins implicated in the regulation of secretory and endocytic vesicle trafficking (Lam et al., 2008; Wang et al., 2010). Antibodies raised against Arabidopsis KNOLLE and ARF1 GTPase, and rice (*Oryza sativa*) SCAMP, labeled similar proportions of wild-type and *pan* mutant SMC cell plates at stages i and ii, with anti-KNOLLE and anti-SCAMP also labeling stage iii plates (Fig. 3, B–D). Arabidopsis Patellin1 (PATL1) is another putative regulator of vesicle formation, which localizes to cell plates at relatively late stages (Peterman et al., 2004). Anti-PATL1 labeled wild-type and *pan* mutant SMC cell plates similarly, predominantly at stage iii (Fig. 3E). Finally, we examined callose via aniline blue staining. Cell plates are initially rich in callose, but callose is replaced with cellulose as cell plates mature (Samuels et al., 1995; Chen et al., 2009). Similar callose staining patterns were observed in wild-type and *pan* SMC cell plates at stages iii and iv (Fig. 3F). Sample images illustrating the localization of all five markers at each stage of SMC cell plate development in each genotype are presented in Supplemental Figure S4. In summary, these experiments indicate that the timing of the recruitment and removal of all cell plate components investigated is similar in *pan* mutant SMC plates compared with the wild type. Together, our studies revealed no requirement for PAN1 in any aspect of cell plate formation.

PAN2 Is Required for Coordinated Shape Changes in Stomatal Subsidiaries and Interstomatal Cells

Like *pan1*, functions for *pan2* outside of SMCs are suggested by its expression in a variety of tissues where no developing stomata are present, including elongating internodes, shoot apices, tassel primordia, and early embryos (Sekhon et al., 2011). Indeed, a function for *pan2*

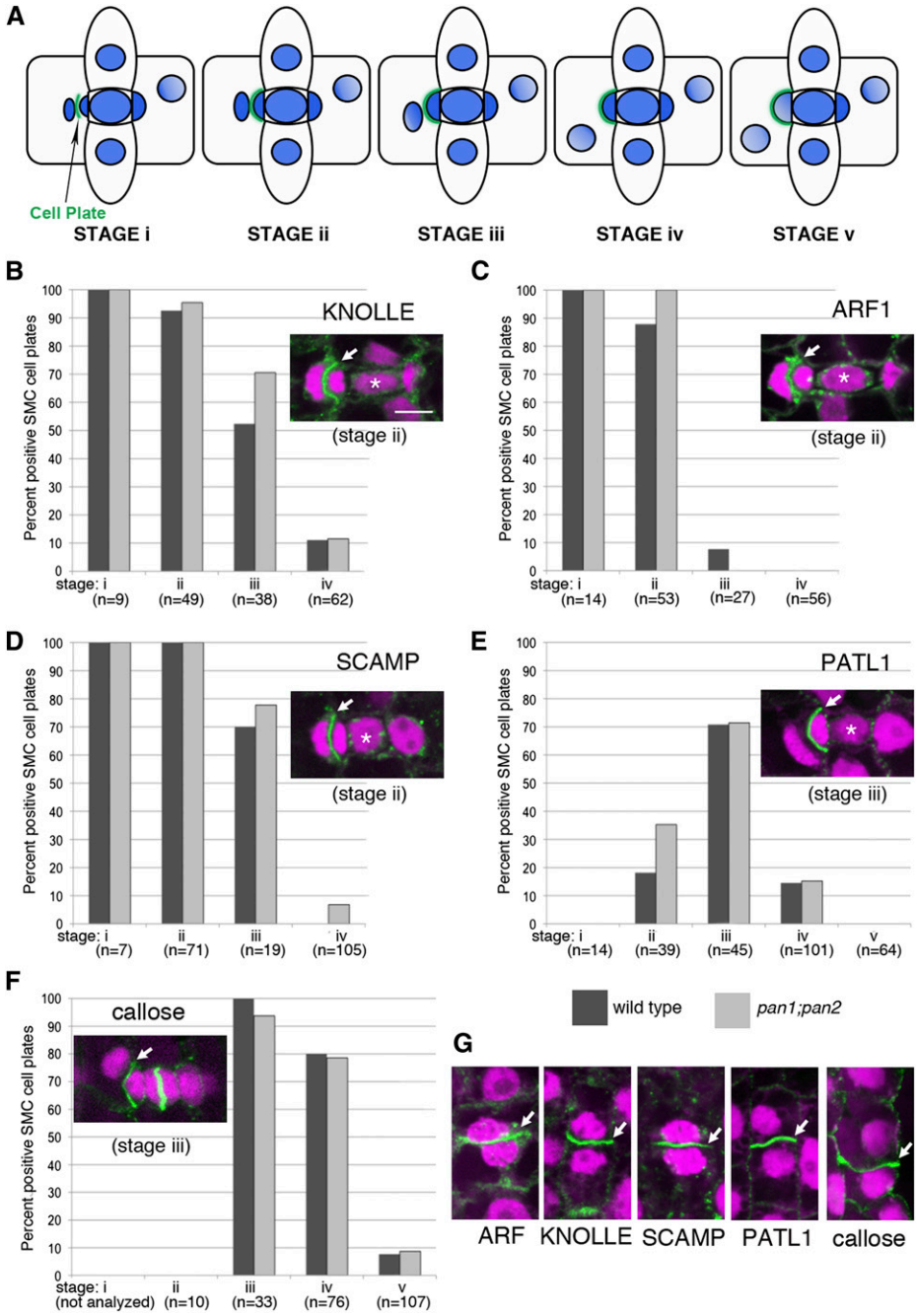

Figure 3. Analysis of cell plate markers in wild-type versus *pan1;pan2* mutant cell plates. A, Schematic illustration of the stages of SMC cytokinesis defined for this analysis. At stages i and ii, both daughter nuclei are condensed. At stage i, the cell plate is not yet fully attached, whereas at stage ii, it is fully attached to the mother cell wall. Stages iii, iv, and v are distinguished by the positions and degrees of condensation of daughter nuclei as illustrated (with darker blue and smaller size indicating a higher degree of SMC daughter nuclei condensation). B to F, Representative images of SMC cell plate labeling and the proportion of SMC cell plates at each stage (among *n* examined as indicated) in the wild type (dark gray bars) versus the *pan1;pan2* double mutant (light gray bars) labeled with anti-KNOLLE (B), anti-ARF1 (C), anti-SCAMP (D), anti-PATL1 (E), and aniline blue (F). The results indicate that the timing of the recruitment and removal of these cell plate markers is similar in mutant SMC plates compared with the wild type. G, Sample images showing cell plates in symmetrically dividing leaf epidermal cells labeled with the same reagents used in B to F, further illustrating the specificity of each label for cell plates. Bar = 10 μm for all images.

in postmitotic cell morphogenesis is indicated by the observation that *pan2* mutant stomata have a striking shape difference compared with wild-type or *pan1* mutant stomata (Fig. 4, A–C). Stomata in wild-type leaves are composed of a guard cell pair flanked by a pair of triangular subsidiary cells, which are the products of asymmetric SMC divisions. Figure 4A illustrates stomatal morphogenesis in wild-type leaves via a series of images acquired at the same magnification, with stage 1 immediately following the completion of asymmetric SMC cytokinesis and stage 5 representing fully expanded stomata. As previously described (Panteris et al., 2007; Giannoutsou et al., 2011), these images reveal that the triangular shape of wild-type subsidiary cells results from extremely unequal elongation of the subsidiary wall segments present at stage 1. The wall segment produced by asymmetric SMC cytokinesis, with one example highlighted in red and labeled wall "y" in Figure 4A, does not elongate at all from stage 1 to stage 5 and becomes one of three points defining the triangular subsidiary shape (Fig. 4, A and E). In contrast, the wall segment joining wall y to the guard cell, highlighted in yellow and

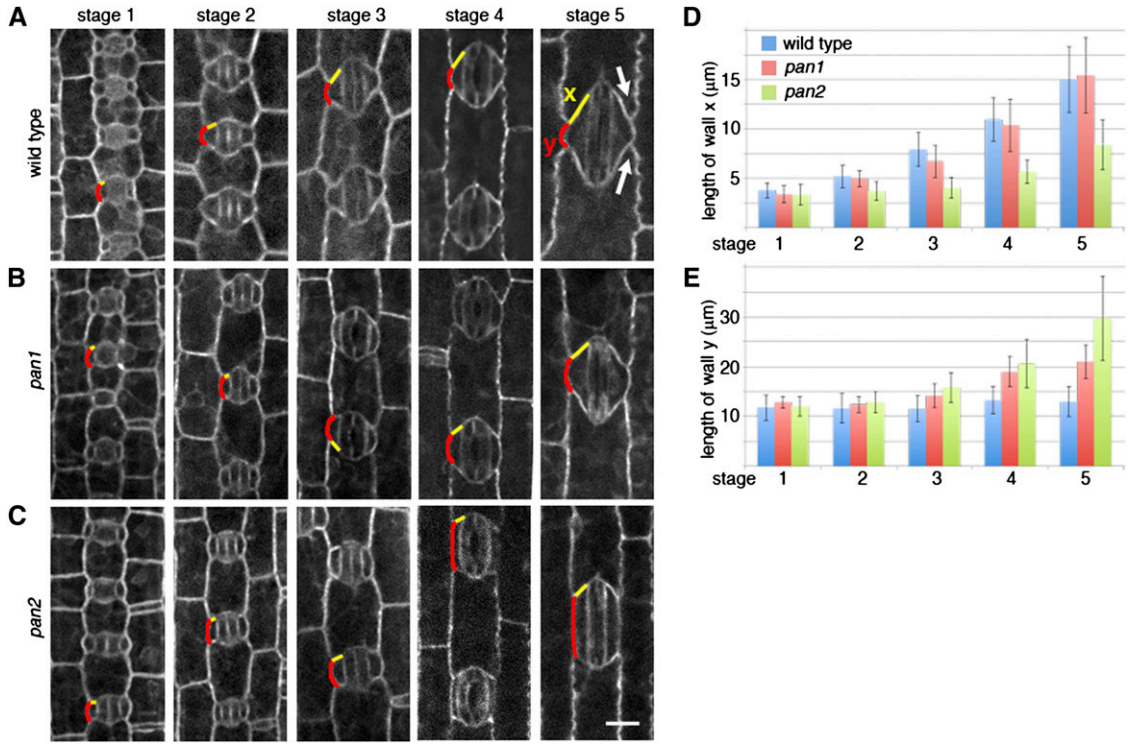

Figure 4. Analysis of stomatal morphogenesis in the wild type versus *pan* mutants. A to C, Midplane confocal slices through the epidermal layer of leaves of the indicated genotypes expressing YFP-tubulin to permit the visualization of cell outlines. Stomatal morphogenesis is divided into five stages. At stage 1, subsidiary cells have just formed; at stage 5, all cells are fully expanded. All images are shown at the same magnification to illustrate how cell shapes change as they expand. The wall produced by asymmetric cytokinesis in SMCs is defined as wall y, and one example in each image is highlighted in red. The subsidiary wall segment linking wall y to the guard cells is defined as wall x, with one example in each image highlighted in yellow. Arrows in the stage 5 wild-type image indicate points that form on the ends of interstomatal cells as subsidiary cells acquire a triangular shape. Bar = 14 μm for all images. D and E, Analysis of the lengths of wall x (D) and wall y (E) at each stage of stomatal morphogenesis in plants of the indicated genotypes (n = 24–45 cells analyzed at each stage for each genotype; error bars show SD). The altered shapes of subsidiary cells in *pan2* mutants result from increased elongation of wall y and decreased elongation of wall x.

labeled wall "x" in Figure 4A, elongates extensively, as does the wall shared by the subsidiary and neighboring guard cell (Fig. 4, A and D). In concert with the acquisition of triangular shape in subsidiary cells, points are formed on the ends of adjacent interstomatal cells (Fig. 4A, stage 5, arrows), indicating more rapid elongation of the interstomatal wall segment shared with subsidiary cells compared with that shared with guard cells.

When SMC divisions are oriented correctly, subsidiary cell shapes in *pan1* and *pan2* mutants are indistinguishable from the wild type at birth (Fig. 4, compare stage 1 in B and C with that in A). At maturity, *pan1* mutant subsidiary cell shapes differ slightly from the wild type, with minor flattening of the point made by wall segment y associated with increased elongation of that segment (Fig. 1, B and E). In contrast, the shapes of *pan2* subsidiary cells at maturity are dramatically different from the wild type, with long, flat sides produced by greatly increased elongation of wall y and reduced elongation of wall x compared with the wild type (Fig. 4, C–E). The points on the ends of *pan2* interstomatal cells are correspondingly reduced (Fig. 4C). Only 20% to 30% of *pan2* mutant SMCs divide aberrantly (Zhang et al., 2012), but all *pan2* subsidiary cells exhibit this shape abnormality (only the products of normally oriented SMC divisions are shown in Fig. 4). Thus, the *pan2* subsidiary cell and interstomatal cell shape defects described here arise after the completion of SMC division, are fully penetrant, and are separate from the occasional defects in subsidiary shape resulting from aberrantly oriented divisions.

These observations raise the question of where PAN2 functions to regulate the morphogenesis of stomatal and interstomatal cells and how its localization in these cells may differ from that of PAN1. PAN1-YFP is barely detectable in expanding subsidiary and interstomatal cells, and virtually all detectable signal is at the subsidiary cell-guard cell interface (Fig. 5A). Consistent with a larger role in cell morphogenesis, PAN2-YFP expression levels remain higher overall throughout the period of epidermal cell expansion, with robust YFP signal observed at the surfaces of all cells (Fig. 5B). Notably, the

strongest PAN2-YFP signal is observed along the wall shared by subsidiary and interstomatal cells (Fig. 5B, arrowheads), a rapidly elongating wall segment. Quantitative analysis of PAN2-YFP fluorescence intensities at positions marked a, b, and c in Figure 5B revealed enrichment of 3.7-fold at position a versus b and 2.4-fold at position a versus c ($n = 32$ cells analyzed). Interestingly, plasmolysis of cells via brief treatment with 0.7 M Suc to separate subsidiary and interstomatal cell membranes clearly revealed that the PAN2-YFP enrichment is at the surface of interstomatal cells, not subsidiary cells (Fig. 5C, arrowheads).

PAN2 Promotes Localized Cortical F-Actin Enrichment without Altering Microtubule Organization in Expanding Interstomatal Cells

Since F-actin plays a key role in plant cell expansion and PAN2 promotes the formation of cortical F-actin enrichments in premitotic SMCs (Cartwright et al., 2009), we asked whether PAN2 also promotes the localized accumulation of cortical F-actin during stomatal morphogenesis. To do this, we utilized transgenic plants expressing the second actin-binding domain of fimbrin tagged at both ends with YFP driven from the native fimbrin promoter (http://maize.jcvi.org/cellgenomics/geneDB_report.php?search=1015). This live-cell actin marker was imaged in expanding subsidiaries and interstomatal cells of the wild type and both *pan* mutants. Similar to PAN2-YFP, cortical F-actin was found to be enriched at the interface between subsidiary cells and interstomatal cells, and plasmolysis showed that this enrichment is in the interstomatal cells (Fig. 6A, arrowheads; a quantitative analysis of enrichment at position a versus b and position a versus c is shown in Fig. 6D). This finding is in agreement with previous observations of F-actin distribution in expanding subsidiary and interstomatal cells of maize visualized via phalloidin staining of fixed cells (Panteris et al., 2007; Giannoutsou et al., 2011). Actin enrichment at the subsidiary cell-interstomatal interface was slightly reduced in *pan1* mutants, where cell shapes are subtly altered, but this reduction was not statistically significant (Fig. 6, B and D). In contrast, cortical F-actin enrichment at the subsidiary-interstomatal cell interface was significantly reduced in *pan2* mutants, where cell shapes are more substantially altered (Fig. 6, C and D). Thus, PAN2-YFP enrichment at the interstomatal-subsidiary cell interface is associated with a corresponding enrichment of cortical F-actin, and this F-actin enrichment is significantly reduced in *pan2* mutants, where the elongation of this wall segment is also reduced. These findings suggest that PAN2-dependent actin accumulation at the corners of interstomatal cells drives the acquisition of a triangular shape in the adjacent subsidiary cells.

Microtubules are also an important determinant of plant cell shape, due at least in part to their influence on patterns of cellulose deposition (Szymanski and Cosgrove, 2009). In a situation potentially similar to the one investigated here, cortical microtubules are depleted in epidermal pavement cells at sites of actin enrichment where lobes are emerging, and they form parallel arrays at lobe sinuses where cell expansion is constrained (Fu et al., 2005, 2009; Lin et al., 2013). To investigate the role of microtubules in subsidiary and interstomatal cell morphogenesis in maize, we imaged YFP-α-tubulin (Mohanty et al., 2009) in these cells at multiple stages of growth in the wild type and *pan* mutants. A fan-like arrangement of microtubules associated with the acquisition of triangular shape in expanding wild-type subsidiary cells is lost in *pan2* but not in *pan1* (Supplemental Fig. S5). However, we observed no consistent arrangement of microtubules related to the emergence of points at the ends of interstomatal cells and no obvious difference in microtubule organization in expanding interstomatal cells of the wild type and either *pan* mutant (Supplemental Fig. S5). Thus, we found no evidence of an influence of PAN1 or PAN2 on microtubule organization in expanding interstomatal cells.

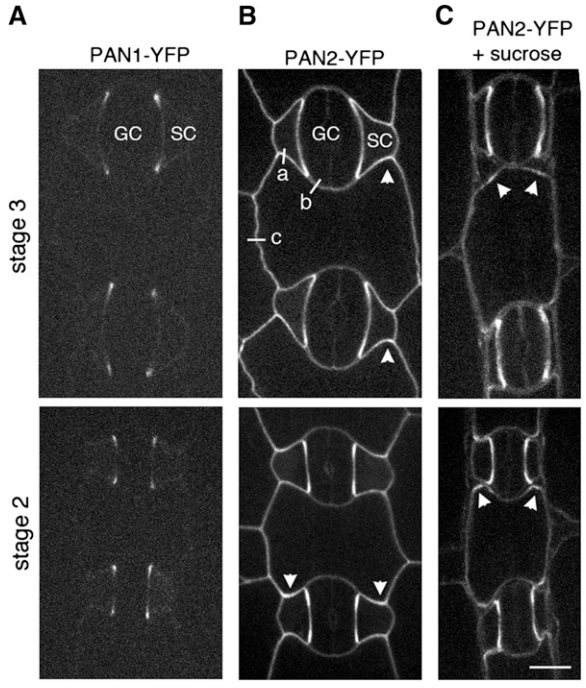

Figure 5. Enrichment of PAN2-YFP in points that emerge at the corners of interstomatal cells. Stages illustrated refer to those defined in Figure 6. Guard cells and subsidiary cells are labeled GC and SC, respectively. A, PAN1-YFP is expressed weakly at the developmental stages illustrated, and almost all detectable signal is found at the interface between subsidiary cells and guard cells. B, PAN2-YFP is detectable at the surfaces of all cells but is enriched at the interface between interstomatal cells and subsidiary cells (arrowheads), reaching a maximum signal intensity at the position marked a. Fluorescence intensity values at positions a, b, and c were analyzed quantitatively as described in the text. C, Tissues were mounted in 0.7 M Suc to achieve the separation of subsidiary and interstomatal cell surfaces, revealing PAN2-YFP enrichments in interstomatal cells (arrowheads). Bar = 10 μm for all images.

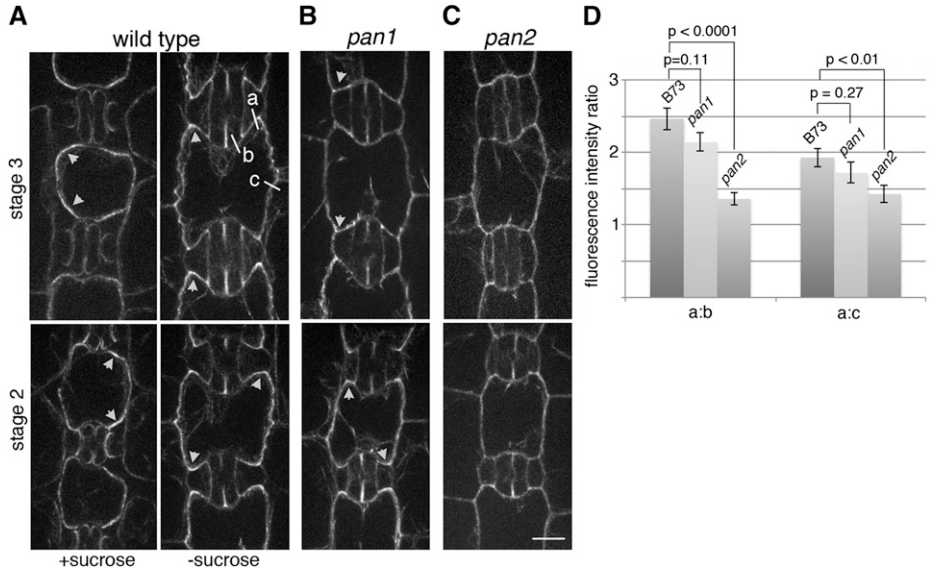

Figure 6. Cortical F-actin enrichment at the corners of interstomatal cells is reduced in *pan2* mutants. A to C, YFP-ABD2-YFP labeling illustrates the distribution of F-actin in expanding stomata and interstomatal cells at stages 2 and 3 in the wild type (A), *pan1* (B), and *pan2* (C). Arrowheads in A and B point to areas of cortical F-actin enrichment seen at the interface between interstomatal cells and subsidiary cells in the absence of Suc. Mounting of wild-type tissue in 0.7 M Suc to achieve separation between subsidiary and interstomatal cells reveals that these cortical F-actin enrichments are in the interstomatal cells (arrowheads). D, Quantitative analysis of YFP-ABD2-YFP signal intensity ratios at position a versus b and position a versus c as defined in A (n = 34–42 cells analyzed per genotype; error bars show SE). P values illustrate the significance of the differences seen for each *pan* mutant relative to the wild type obtained via Student's t test. Cortical F-actin enrichment at interstomatal cell corners is significantly reduced ($P < 0.01$) in *pan2* but not in *pan1*.

Nonuniform Distributions of PIN1-YFP and YFP-ROP2 in Expanding Interstomatal and Subsidiary Cells Are PAN2 Independent

Since polarized localization of PIN1 auxin transporters is implicated in the mechanism of nonuniform cell expansion in epidermal pavement cells (Xu et al., 2010), we wondered whether PIN1 polarization in expanding subsidiary or interstomatal cells of maize is associated with nonuniform expansion in these cells. To investigate this possibility, we analyzed the localization of native promoter-driven PIN1-YFP (ZmPIN1a-YFP; Gallavotti et al., 2008). PIN1a-YFP is uniformly distributed around the periphery of interstomatal cells at all stages of subsidiary morphogenesis in the wild type (Fig. 7A) and both *pan* mutants (Fig. 7, B and C). Although initially almost undetectable at the subsidiary cell face created by asymmetric SMC division (defined in Figure 4 as wall y), PIN1a-YFP rapidly becomes highly enriched at this nonelongating face of wild-type subsidiary cells and remains so throughout all subsequent stages of subsidiary expansion (Fig. 7A, arrowheads). This association of PIN1a with the nonelongating portion of the subsidiary cell surface is the opposite of what has been observed in expanding Arabidopsis pavement cells, where PIN1 and cortical F-actin are both enriched at sites of lobe outgrowth (Xu et al., 2010). However, the significance of PIN1a polarization in expanding maize subsidiary cells is unknown. Remarkably, in spite of the increased elongation of wall y in *pan* mutants, PIN1a-YFP remains highly polarized toward this portion of the cell surface in expanding *pan1* and *pan2* mutant subsidiary cells, localizing as a patch (or a focused chain of dots) at the center of this cell face as it elongates (Fig. 7, B and C, arrowheads). Thus, spatial cues mediating PIN1a targeting must still be present in *pan* mutant subsidiaries, albeit uncoupled from wall elongation control.

Finally, continuing to explore possible parallels with pavement cell lobe formation, where ROPs play a key role in regulating both cortical F-actin polymerization and microtubule organization related to the emergence of epidermal lobes (Fu et al., 2005, 2009; Lin et al., 2013), we investigated the localization of YFP-ROP2 (described by Humphries et al., 2011) in expanding subsidiary and interstomatal cells in maize and its dependence on PAN2. ROP2 is of further interest here because PAN1 was found to physically interact with, and function cooperatively with, type I ROPs to polarize SMC divisions (Humphries et al., 2011). PAN2 acts upstream of PAN1 in SMC polarization, so its function in these cells is also related to type I ROPs, but a physical interaction between PAN2 and ROP2 or other type I ROPs has not been demonstrated. YFP-ROP2 appears relatively uniform in its distribution at the surface of expanding subsidiary cells in both the wild type and *pan2* mutants (Fig. 8, A and B). YFP-ROP2 is conspicuously depleted at the interface between interstomatal cells and guard cells

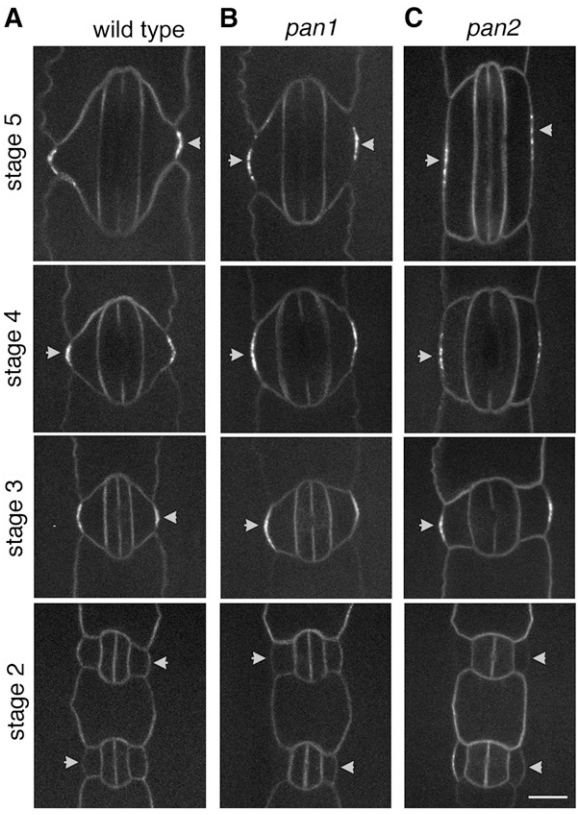

Figure 7. PAN1- and PAN2-independent polarization of ZmPIN1a-YFP in expanding subsidiary cells. All images are shown at the same magnification to illustrate cell enlargement at successive stages of stomatal morphogenesis, numbered as illustrated in Figure 4. Arrowheads point to subsidiary cell surface segment y produced by the asymmetric cytokinesis of subsidiary mother cells. ZmPIN1a-YFP becomes polarized toward this segment of the cell surface shortly after its formation in the wild type (A). In *pan1* (B) and especially in *pan2* (C), where wall segment y elongates more than in the wild type, ZmPIN1a-YFP remains concentrated at the center of this segment, maintaining a polarized distribution similar to that seen in the wild type. Bar = 10 μm for all images.

(interface b in Fig. 8A) but is otherwise uniformly distributed around the periphery of expanding interstomatal cells, with no enrichment at the interface with subsidiary cells (interface a in Fig. 8A; a quantitative analysis of signal intensity ratios confirming these conclusions is shown in Fig. 8C). The nonuniform distribution of YFP-ROP2 at the interstomatal cell surface does not appear related to the role of PAN2 in the morphogenesis of these cells, since no difference was observed in YFP-ROP2 distribution in wild-type versus *pan2* mutant cells (Fig. 8, B and C). Thus, we find no evidence that PAN2 acts through ROP2 to promote localized cortical F-actin accumulation and nonuniform cell expansion.

DISCUSSION

Prior studies have demonstrated a cooperative function for PAN1 and PAN2 in the polarization of SMC divisions during stomatal development in maize and a dependence of PAN1 on PAN2 for its polarized localization in premitotic SMCs (Cartwright et al., 2009; Zhang et al., 2012). The work presented here demonstrates unequal or divergent roles for PAN1 and PAN2 in other developmental processes.

PAN1 is enriched at developing cell plates, not only in SMCs but in all dividing cell types examined. Unlike the situation in premitotic SMCs, PAN1 does not depend on PAN2 for its localization to cell plates, consistent with a lack of detectable PAN2 at cell plates. In further contrast to the situation in SMCs, PAN1 function in cell plates could not be linked to F-actin polymerization, since no difference in phragmoplast- or cell plate-associated F-actin was observed in *pan* mutants. Analysis of cytokinesis in *pan* mutants did not reveal a unique role for PAN1 in cell plate formation. The frequent misorientation of cell plates in *pan1* mutant SMCs raises the possibility that PAN1 may function in attachment of the cell plate to the mother cell wall rather than in cell plate formation or maturation, as demonstrated for the cell plate-localized, putative vesicle-trafficking regulator TPLATE (Van Damme et al., 2006, 2011). However, cell plate misorientation is only observed

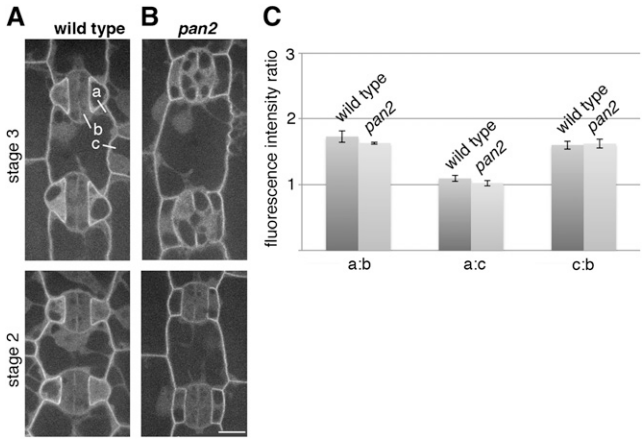

Figure 8. YFP-ROP2 localization in expanding stomata and interstomatal cells. A and B, The wild type (A) and the *pan2* mutant (B) at stage 2 (bottom) and stage 3 (top). YFP-ROP2 distribution was not analyzed in *pan1* mutants because there was very little difference in the shapes of subsidiary and interstomatal cells in *pan1* mutants compared with the wild type. The distribution of YFP-ROP2 on subsidiary versus interstomatal cell surfaces could not be determined via plasmolysis experiments, because YFP-ROP2 signal was lost very rapidly from the cell surface in the presence of Suc at concentrations sufficient to cause plasmolysis. Bar = 10 μm for all images. C, Ratios of fluorescence intensities measured at positions a, b, and c as marked in A ($n \geq 25$ cells analyzed per genotype). Error bars show SE. In both genotypes and stages, a modest enrichment of YFP-ROP2 was observed at positions a and c relative to position b. However, in contrast to YFP-ABD2-YFP and PAN2-YFP, no enrichment of YFP-ROP2 was evident at position a versus position c. Moreover, no significant difference was observed in any of the measured ratios when comparing the wild type versus the *pan2* mutant ($P > 0.2$ by Student's *t* test for all three comparisons).

in SMCs, even though PAN1 is localized to cell plates in all classes of dividing cells, arguing against this possibility and in favor of the idea that cell plate misorientation in both *pan1* and *pan2* mutant SMCs results from defects in premitotic SMC polarity instead. There may be a subtle defect in cell plate development in *pan* mutants that could be revealed by an analysis of additional molecular markers or of the timing of cell plate expansion or attachment. An alternative and likely possibility, in view of the large number of closely related LRR-RLKs present in maize as in other plants, is that functional redundancy between PAN1 and one or more additional LRR-RLKs conceals the functional significance of cell plate-localized PAN1. In any case, the observation of an LRR-RLK at the cell plate is interesting because it suggests ligand-mediated regulation of some aspect of cell plate or phragmoplast development. Thus, the interaction of LRR-RLKs such as PAN1 with ligands produced inside the cell plate as early steps in plate biogenesis are completed may regulate the progression of cell plate formation (e.g. by triggering the recruitment of later-acting cell plate components).

Our study also showed that PAN2 plays a greater role than PAN1 in the coordinated morphogenesis of stomatal subsidiary and interstomatal cells after the completion of stomatal divisions. PAN2 is enriched at the surfaces of expanding interstomatal cells, where they contact subsidiary cells, and stimulates a corresponding enrichment of cortical F-actin there. In *pan2* mutants, reduced F-actin accumulation at this face of expanding interstomatal cells is associated with a failure of points to emerge at the ends of these cells and with a concomitant failure of neighboring subsidiary cells to acquire a triangular shape. Thus, as in SMCs, PAN2 function in interstomatal cell morphogenesis is closely tied to localized actin polymerization. In premitotic SMCs, PAN2 is linked to localized actin polymerization via PAN1 and type I ROP GTPases (Cartwright et al., 2009; Humphries et al., 2011). However, in expanding interstomatal cells, we find no enrichment of PAN1 or ROP2 at the interface with subsidiary cells where PAN2 and F-actin are enriched, and analysis of *pan1* mutants demonstrates only a very minor role for PAN1 in interstomatal and subsidiary cell morphogenesis. Thus, PAN2 appears to be linked to actin polymerization via a different mechanism in interstomatal cells compared with SMCs, and this mechanism remains to be elucidated.

Fine actin filament networks at or near the plasma membrane are associated with localized expansion of the cell surface in tip-growing cells (Vidali et al., 2001; Cárdenas et al., 2008; Dong et al., 2012) and expanding pavement cells (Frank and Smith, 2002; Fu et al., 2002). In tip-growing cells, the contribution of actin filaments at the growth site has been difficult to separate from that of cytoplasmic actin filament bundles that drive long-range transport of vesicles to and away from the tip, but evidence is accumulating that dynamic actin filament networks at the growth site promote the accumulation and perhaps also the fusion with and/or removal of vesicles from the plasma membrane (Qin and Yang, 2011; Chebli et al., 2013). In pavement cells, cortical F-actin enriched at sites of lobe outgrowth has been implicated in the local suppression of PIN1 endocytosis, thereby promoting the localized enrichment of PIN1, leading to the local accumulation of auxin, which drives localized cell expansion (Nagawa et al., 2012). Thus, although we found no evidence of a similar role for maize PIN1a in interstomatal cell morphogenesis, findings for other cell types exhibiting polarized growth suggest that PAN2-dependent cortical F-actin accumulation in interstomatal cells also promotes localized cell surface expansion via the modulation of membrane and/or vesicle dynamics. This proposal is further supported by the finding that F-actin promotes local aggregation of cortical endoplasmic reticulum at the emerging points on the ends of interstomatal cells, where the endoplasmic reticulum may facilitate membrane-trafficking events supporting localized wall expansion (Giannoutsou et al., 2011).

Perhaps the most interesting facet of our results is the evidence they offer of a non-cell-autonomous influence of interstomatal cells on the morphogenesis of neighboring subsidiary cells. Specifically, PAN2 and actin function at the interstomatal cell surface contacting subsidiary wall x (as defined in Fig. 4) suppresses the elongation of subsidiary wall y. The enlargement of subsidiary cells in step with the neighboring guard cells cannot occur without the elongation of subsidiary wall x and/or y. Thus, redirection of growth to wall y in *pan2* mutant subsidiary cells may be a response to the lack of elongation of wall x, potentially mediated by the perception of physical forces such as wall or membrane tension. Given the role of physical forces in orienting microtubules in plant cells (Landrein and Hamant, 2013), this idea is consistent with our observation that the altered growth pattern in *pan2* mutant subsidiary cells is associated with an alteration in microtubule organization in these cells. It is interesting that excess elongation of wall y occurs in *pan2* mutant subsidiary cells in spite of the correct localization of PIN1a to the center of this cell face, likely requiring continuous spatial regulation of membrane recycling to maintain PIN polarity, as in other cell types (Feraru and Friml, 2008). Thus, our findings suggest that some aspects of polarized membrane trafficking are preserved in expanding *pan2* subsidiary cells (those required for PIN1a targeting) while others are altered (those normally producing preferential elongation of wall x relative to y). Finally, in view of the putative function of PAN2 as a receptor and the need for coordination of cell expansion between interstomatal and subsidiary cells, it is interesting to consider the possibility that the subsidiary cell produces a ligand to which PAN2 in the adjoining interstomatal cell responds by promoting localized actin polymerization and cell surface expansion. Thus, we speculate that receptor-mediated cell-cell interaction, as well as physical forces, mediate the normal distribution of growth to different wall segments to achieve locally coordinated cell shape changes during epidermal development.

The findings reported here reveal that PAN1 and PAN2 have other functions in addition to their shared function in the premitotic polarization of SMCs. Adding further to this conclusion, the closest relative of PAN2 in Arabidopsis was recently identified as Guard Cell Hydrogen Peroxide Resistant1, which regulates guard cell aperture in mature leaves in response to abscisic acid and hydrogen peroxide (Hua et al., 2012). In playing multiple roles, PANs are similar to other receptors such as FERONIA (Cheung and Wu, 2011) and members of the ERECTA (van Zanten et al., 2009) and SERK (Chinchilla et al., 2009; Li, 2010) families in Arabidopsis. For example, ERECTA partners with closely related LRR-RLKs (ERECTA-LIKE proteins) to mediate intercellular signaling controlling the occurrence and orientation of asymmetric stomatal divisions (Pillitteri and Torii, 2012), promotes axis elongation and normal morphogenesis of multiple aerial organs (van Zanten et al., 2009), and increases resistance to bacterial and fungal pathogens (Godiard et al., 2003; Llorente et al., 2005). Our finding of previously unrecognized roles for PAN1 and PAN2 demonstrates that these receptor-like proteins are not dedicated to the perception of GMC-derived polarizing cues but also participate in cell plate development (PAN1) or polarized cell growth (mainly PAN2). We propose that PANs may function in all contexts in the polarization of membrane trafficking, either directly or indirectly via their influence on actin polymerization. The central importance of membrane trafficking in cell plate formation and polarized cell growth is well established, as discussed earlier. The spatial regulation of membrane trafficking has not been shown to play an essential role in the polarization of plant cell division but generates the polarized distribution of a variety of proteins in both plant and animal cells (Feraru and Friml, 2008; Apodaca et al., 2012). Thus, an important role for polarized membrane trafficking in the polarization of plant cell division is plausible.

MATERIALS AND METHODS

Plants and Growth Conditions

All maize (*Zea mays*) mutants employed in this study have been described previously. Analysis of cytokinesis defects in *pan* mutants utilized *pan1-Mu* (Gallagher and Smith, 2000), *pan1-ems* (Cartwright et al., 2009), and *pan1-Mu; pan2-O* (Zhang et al., 2012) double mutants. Analysis of subsidiary and interstomatal morphogenesis defects utilized *pan1-ems* (Cartwright et al., 2009) and *pan2-2* (Zhang et al., 2012) mutants. All mutants were backcrossed two or more times into the B73 wild-type background and compared with inbred B73 as the wild type. Transgenic plants expressing native promoter-driven PAN1-YFP, YFP-ROP2, and PAN2-YFP were described previously (Humphries et al., 2011; Zhang et al., 2012). Transgenics expressing native promoter-driven CFP-β-tubulin, YFP-α-tubulin, 2XYFP-ABD2 (the second actin-binding domain of fimbrin tagged at both ends with YFP), and ZmPIN1a-YFP were generated as described by Mohanty et al. (2009) and at http://maize.jcvi.org/cellgenomics/index.php and were generously provided by Anne Sylvester (University of Wyoming). All transgenes were backcrossed two or more times to B73 and introduced into mutant backgrounds via crossing to mutants in the B73 background. YFP- and CFP-tagged proteins were imaged in live cells after mounting tissues in distilled water. For imaging and phenotypic analysis, plants were grown for 10 d to 4 weeks in a greenhouse maintained between 60°F and 90°F with natural lighting year round in La Jolla, California. Analysis of cell plate localization and cytokinesis phenotypes utilized juvenile leaves (leaf 3 or 4); analysis of protein localization and cell morphology defects in stomatal subsidiaries and interstomatal cells utilized adult leaf 8.

Staining of Actin, Callose, Cell Walls, and Nuclei

To analyze *pan* mutants for cytokinesis defects, mature blade tissue from leaf 3 or 4 was fixed and stained with acriflavine or 100 μg mL^{-1} propidium iodide as described previously (Cleary and Smith, 1998; Hunter et al., 2012) and mounted in water (after propidium iodide staining) or saturated chloral hydrate (after acriflavine staining) for imaging of epidermal walls and nuclei via confocal microscopy.

To stain callose in cell plates, the basal-most 2 cm of leaf 3 or 4 was cut into 2-cm-long × 2- to 3-mm-wide strips and fixed with formalin-acetic acid for 1 h. Following rehydration, tissues were stained with 0.1% (w/v) aniline blue in KPO_4 buffer at pH 11 for 30 min, rinsed in phosphate-buffered saline, stained with 10 μg mL^{-1} propidium iodide to label nuclei, rinsed again, and mounted in Vectashield (Vector Laboratories) for imaging via confocal microscopy.

To label phragmoplast actin, the basal 2 cm of leaf 3 or 4 was cut into strips 2 cm long × 2 to 3 mm wide, fixed, and stained with Alexa Fluor 488-conjugated phalloidin (Invitrogen) as described previously (Cartwright et al., 2009). Propidium iodide at 10 μg mL^{-1} was used to stain nuclei. Samples were mounted in Vectashield (Vector Laboratories) for imaging via confocal microscopy.

Immunolocalization and Protein Gel Blotting

All antibodies used in this study were characterized previously. Anti-PAN1 (Cartwright et al., 2009) and anti-PAN2 (Zhang et al., 2012) were generated in our laboratory. Anti-SCAMP (Lam et al., 2007) was raised against a rice (*Oryza sativa*) SCAMP protein whose closest relative in maize is GRMZM2G041181 and was provided by Liwen Jiang (Chinese University of Hong Kong). Anti-KNOLLE (Lukowitz et al., 1996) was raised against the Arabidopsis (*Arabidopsis thaliana*) KNOLLE protein, whose closest relative in maize is GRMZM2G100478, and was provided by Gerd Jurgens (University of Tuebingen). Anti-PATL1 (Peterman et al., 2004) was raised against Arabidopsis PATL1, whose closest relative in maize is GRMZM2G081652, and was provided by Kaye Peterman (Wellesley College). Anti-ARF1 was raised against Arabidopsis ARF1, whose closest relatives in maize are GRMZM2G105996, GRMZM2G357399, and GRMZM5G836182. This antibody was purchased from Agrisera and is described at the product Web page (http://www.agrisera.com/en/artiklar/plant_algal-cell-biology/compartment-markers/plant-Golgi-marker/arf1-adp-ribosylation-factor-1.html).

For tests of antibody specificity via protein gel blotting, proteins were extracted from the basal 2 cm of leaves of 3- to 4-week-old B73 maize plants after removal of leaves with expanded sheaths. Membrane and soluble fractions were prepared, separated via SDS-PAGE, and analyzed via immunoblotting as described previously (Cartwright et al., 2009). For immunolocalization, the basal 2 cm of leaf 3 or 4 (containing cells at all stages of stomatal development) was excised from 10- to 20-d-old plants, cut into strips 2 cm long × 2 to 3 mm wide, fixed, and stained via a whole-mount procedure described previously (Cartwright et al., 2009). Primary antibodies were used for immunolocalization at the following dilutions: affinity-purified anti-PAN1 and anti-PAN2 at 2 μg mL^{-1}, anti-ARF1 serum diluted to 1:2,000, affinity-purified anti-SCAMP at 1.5 μg mL^{-1}, anti-KNOLLE serum diluted to 1:1,000, and anti-PATL1 serum diluted to 1:1,000. Binding of anti-KNOLLE, anti-ARF1, anti-SCAMP, and anti-PATL1 antibodies was visualized by labeling with Alexa Fluor 488-conjugated secondary antibodies (Invitrogen) diluted 1:200. Binding of anti-PAN1 and anti-PAN2 was visualized using Invitrogen Tyramide Signal Amplification kit 12 following the manufacturer's instructions. Nuclei were subsequently counterstained with 10 μg mL^{-1} propidium iodide (Sigma). Tissues were mounted in Vectashield (Vector Laboratories) and imaged via confocal microscopy as described below.

Confocal Microscopy and Image Analysis

Confocal imaging of fluorescence labeling was performed using a custom-assembled spinning-disk microscope system described previously (Walker et al., 2007). YFP-tubulin images for subsidiary cell shape analysis were acquired with a Nikon 20× dry objective, and all other images were acquired with a Nikon 60× water-immersion objective. Alexa Fluor 488 was excited with an argon laser (488-nm line) and visualized with a Chroma HQ525/60 emission filter. Propidium iodide was excited with an argon/krypton laser (568-nm line) and visualized with a Chroma HQ620/60 filter. YFP was excited with 514 nm and viewed with a Chroma HQ570/65 emission filter. CFP and

aniline blue were excited with a 440-nm laser and viewed with a Chroma HQ525/50 emission filter. Z projections of image stacks were produced using ImageJ version 1.36b or 1.47g (http://rsb.info.nih.gov/ij/). Further image processing (adjustment of black levels, brightness, and contrast, production of color merges, and figure preparation) was carried out using Adobe Photoshop version 8.0 or 11.02, applying only linear adjustments to pixel values.

For quantitative analysis of PAN2-YFP, YFP-ABD2-YFP, and YFP-ROP2 signal intensities, ImageJ version 1.47g was used to measure fluorescence intensities along the length of a line drawn at positions a, b, and c as indicated in Figures 5, 6, and 8 on Z projections of a standard number of focal planes for each marker. Minimum fluorescence intensity values (background signal) were subtracted from maximum values, and ratios of these background-subtracted maximum values (a to b and a to c) were calculated for individual cells at stages 2 or 3 as defined in Figure 4 (one set of measurements per cell). For PAN2-YFP analysis, 32 cells from 13 different wild-type individuals expressing PAN2-YFP were analyzed. For YFP-ABD2-YFP, we analyzed 42 cells from two wild-type individuals, 34 cells from two *pan2* mutant individuals, and 42 cells from two *pan1* mutant individuals. For YFP-ROP2, we analyzed 29 cells from three wild-type individuals and 25 cells from three *pan2* individuals.

Quantitative analysis of PAN1-YFP intensities in SMCs (Fig. 2, I and J) was conducted similarly except that single focal planes were used, and lines were drawn through the cell plate and the GMC contact site in SMCs (n = 62 wild type and 72 *pan2*) that had recently completed cytokinesis, as judged by the presence of phragmoplast remnants and nuclear appearance, corresponding to the stage when cell plate-associated PAN1 signal was highest.

Sequences for the genes and proteins investigated in this study can be found at http://www.maizesequence.org (release 5b.60) as GRMZM2G034572_T01 and GRMZM2G034572_P01 (PAN2), GRMZM5G836190_T02 and GRMZM5G836190_P02 (PAN1), GRMZM2G098643_T01 and GRMZM2G098643_P01 (PIN1a), and GRMZM5G846811_T01 and GRMZM5G846811_P01 (ROP2).

Supplemental Data

The following materials are available in the online version of this article.

Supplemental Figure S1. PAN1 localization at cell plates of root cortical cells.

Supplemental Figure S2. Analysis of phragmoplast F-actin in wild-type and *pan* mutant SMCs.

Supplemental Figure S3. Protein gel-blot analysis of the specificities of antibodies used in this study.

Supplemental Figure S4. Immunostaining with antibodies to cell plate markers in wild-type and *pan* mutant SMCs undergoing cytokinesis.

Supplemental Figure S5. Microtubule organization visualized via imaging of YFP-α-tubulin in expanding subsidiary and interstomatal cells.

ACKNOWLEDGMENTS

We thank Xiaoguo Zhang for supplying the PAN2 immunolocalization data presented in Figure 2, Anne Sylvester for supplying transgenic lines expressing ZmPIN1a-YFP, CFP-tubulin, YFP-tubulin, and YFP-ABD2-YFP, and Gerd Jurgens, Kaye Peterman, and Liwen Jiang for providing antibodies used in this study.

Received November 15, 2013; accepted February 24, 2014; published February 27, 2014.

LITERATURE CITED

Apodaca G, Gallo LI, Bryant DM (2012) Role of membrane traffic in the generation of epithelial cell asymmetry. Nat Cell Biol **14:** 1235–1243

Boudeau J, Miranda-Saavedra D, Barton GJ, Alessi DR (2006) Emerging roles of pseudokinases. Trends Cell Biol **16:** 443–452

Cárdenas L, Lovy-Wheeler A, Kunkel JG, Hepler PK (2008) Pollen tube growth oscillations and intracellular calcium levels are reversibly modulated by actin polymerization. Plant Physiol **146:** 1611–1621

Cartwright HN, Humphries JA, Smith LG (2009) PAN1: a receptor-like protein that promotes polarization of an asymmetric cell division in maize. Science **323:** 649–651

Castells E, Casacuberta JM (2007) Signalling through kinase-defective domains: the prevalence of atypical receptor-like kinases in plants. J Exp Bot **58:** 3503–3511

Chebli Y, Kroeger J, Geitmann A (2013) Transport logistics in pollen tubes. Mol Plant **6:** 1037–1052

Chen XY, Liu L, Lee E, Han X, Rim Y, Chu H, Kim SW, Sack F, Kim JY (2009) The Arabidopsis callose synthase gene *GSL8* is required for cytokinesis and cell patterning. Plant Physiol **150:** 105–113

Cheung AY, Wu HM (2011) THESEUS 1, FERONIA and relatives: a family of cell wall-sensing receptor kinases? Curr Opin Plant Biol **14:** 632–641

Chinchilla D, Shan L, He P, de Vries S, Kemmerling B (2009) One for all: the receptor-associated kinase BAK1. Trends Plant Sci **14:** 535–541

Cleary AL, Smith LG (1998) The *Tangled1* gene is required for spatial control of cytoskeletal arrays associated with cell division during maize leaf development. Plant Cell **10:** 1875–1888

Couchy I, Bolte S, Crosnier MT, Brown S, Satiat-Jeunemaitre B (2003) Identification and localization of a beta-COP-like protein involved in the morphodynamics of the plant Golgi apparatus. J Exp Bot **54:** 2053–2063

Dong H, Pei W, Haiyun R (2012) Actin fringe is correlated with tip growth velocity of pollen tubes. Mol Plant **5:** 1160–1162

Feraru E, Friml J (2008) PIN polar targeting. Plant Physiol **147:** 1553–1559

Frank MJ, Smith LG (2002) A small, novel protein highly conserved in plants and animals promotes the polarized growth and division of maize leaf epidermal cells. Curr Biol **12:** 849–853

Fu Y, Gu Y, Zheng Z, Wasteneys G, Yang Z (2005) Arabidopsis interdigitating cell growth requires two antagonistic pathways with opposing action on cell morphogenesis. Cell **120:** 687–700

Fu Y, Li H, Yang Z (2002) The ROP2 GTPase controls the formation of cortical fine F-actin and the early phase of directional cell expansion during *Arabidopsis* organogenesis. Plant Cell **14:** 777–794

Fu Y, Xu T, Zhu L, Wen M, Yang Z (2009) A ROP GTPase signaling pathway controls cortical microtubule ordering and cell expansion in Arabidopsis. Curr Biol **19:** 1827–1832

Galatis B, Apostolakos P (2004) The role of the cytoskeleton in the morphogenesis and function of stomatal complexes. New Phytol **161:** 613–639

Gallagher K, Smith LG (2000) Roles for polarity and nuclear determinants in specifying daughter cell fates after an asymmetric cell division in the maize leaf. Curr Biol **10:** 1229–1232

Gallavotti A, Yang Y, Schmidt RJ, Jackson D (2008) The Relationship between auxin transport and maize branching. Plant Physiol **147:** 1913–1923

Giannoutsou EP, Apostolakos P, Galatis B (2011) Actin filament-organized local cortical endoplasmic reticulum aggregations in developing stomatal complexes of grasses. Protoplasma **248:** 373–390

Godiard L, Sauviac L, Torii KU, Grenon O, Mangin B, Grimsley NH, Marco Y (2003) ERECTA, an LRR receptor-like kinase protein controlling development pleiotropically affects resistance to bacterial wilt. Plant J **36:** 353–365

Hua D, Wang C, He J, Liao H, Duan Y, Zhu Z, Guo Y, Chen Z, Gong Z (2012) A plasma membrane receptor kinase, GHR1, mediates abscisic acid- and hydrogen peroxide-regulated stomatal movement in *Arabidopsis*. Plant Cell **24:** 2546–2561

Humphries JA, Vejlupkova Z, Luo A, Meeley RB, Sylvester AW, Fowler JE, Smith LG (2011) ROP GTPases act with the receptor-like protein PAN1 to polarize asymmetric cell division in maize. Plant Cell **23:** 2273–2284

Hunter CT, Kirienko DH, Sylvester AW, Peter GF, McCarty DR, Koch KE (2012) *Cellulose Synthase-Like D1* is integral to normal cell division, expansion, and leaf development in maize. Plant Physiol **158:** 708–724

Jürgens G (2005) Cytokinesis in higher plants. Annu Rev Plant Biol **56:** 281–299

Lam SK, Cai Y, Hillmer S, Robinson DG, Jiang L (2008) SCAMPs highlight the developing cell plate during cytokinesis in tobacco BY-2 cells. Plant Physiol **147:** 1637–1645

Lam SK, Siu CL, Hillmer S, Jang S, An G, Robinson DG, Jiang L (2007) Rice SCAMP1 defines clathrin-coated, trans-golgi-located tubular-vesicular structures as an early endosome in tobacco BY-2 cells. Plant Cell **19:** 296–319

Landrein B, Hamant O (2013) How mechanical stress controls microtubule behavior and morphogenesis in plants: history, experiments and revisited theories. Plant J **75:** 324–338

Lauber MH, Waizenegger I, Steinmann T, Schwarz H, Mayer U, Hwang I, Lukowitz W, Jürgens G (1997) The Arabidopsis KNOLLE protein is a cytokinesis-specific syntaxin. J Cell Biol **139:** 1485–1493

Li J (2010) Multi-tasking of somatic embryogenesis receptor-like protein kinases. Curr Opin Plant Biol **13:** 509–514

Lin D, Cao L, Zhou Z, Zhu L, Ehrhardt D, Yang Z, Fu Y (2013) Rho GTPase signaling activates microtubule severing to promote microtubule ordering in Arabidopsis. Curr Biol **23:** 290–297

Llompart B, Castells E, Río A, Roca R, Ferrando A, Stiefel V, Puigdomenech P, Casacuberta JM (2003) The direct activation of MIK, a germinal center kinase (GCK)-like kinase, by MARK, a maize atypical receptor kinase, suggests a new mechanism for signaling through kinase-dead receptors. J Biol Chem **278:** 48105–48111

Llorente F, Alonso-Blanco C, Sánchez-Rodriguez C, Jorda L, Molina A (2005) ERECTA receptor-like kinase and heterotrimeric G protein from Arabidopsis are required for resistance to the necrotrophic fungus Plectosphaerella cucumerina. Plant J **43:** 165–180

Lukowitz W, Mayer U, Jürgens G (1996) Cytokinesis in the Arabidopsis embryo involves the syntaxin-related KNOLLE gene product. Cell **84:** 61–71

McMichael CM, Bednarek SY (2013) Cytoskeletal and membrane dynamics during higher plant cytokinesis. New Phytol **197:** 1039–1057

Mohanty A, Luo A, DeBlasio S, Ling X, Yang Y, Tuthill DE, Williams KE, Hill D, Zadrozny T, Chan A, et al (2009) Advancing cell biology and functional genomics in maize using fluorescent protein-tagged lines. Plant Physiol **149:** 601–605

Nagawa S, Xu T, Lin D, Dhonukshe P, Zhang X, Friml J, Scheres B, Fu Y, Yang Z (2012) ROP GTPase-dependent actin microfilaments promote PIN1 polarization by localized inhibition of clathrin-dependent endocytosis. PLoS Biol **10:** e1001299

Panteris E, Galatis B, Quader H, Apostolakos P (2007) Cortical actin filament organization in developing and functioning stomatal complexes of Zea mays and Triticum turgidum. Cell Motil Cytoskeleton **64:** 531–548

Peterman TK, Ohol YM, McReynolds LJ, Luna EJ (2004) Patellin1, a novel Sec14-like protein, localizes to the cell plate and binds phosphoinositides. Plant Physiol **136:** 3080–3094

Pillitteri LJ, Torii KU (2012) Mechanisms of stomatal development. Annu Rev Plant Biol **63:** 591–614

Qin Y, Yang Z (2011) Rapid tip growth: insights from pollen tubes. Semin Cell Dev Biol **22:** 816–824

Rajakulendran T, Sicheri F (2010) Allosteric protein kinase regulation by pseudokinases: insights from STRAD. Sci Signal **3:** pe8

Samuels AL, Giddings THJ Jr, Staehelin LA (1995) Cytokinesis in tobacco BY-2 and root tip cells: a new model of cell plate formation in higher plants. J Cell Biol **130:** 1345–1357

Seguí-Simarro JM, Austin JR II, White EA, Staehelin LA (2004) Electron tomographic analysis of somatic cell plate formation in meristematic cells of *Arabidopsis* preserved by high-pressure freezing. Plant Cell **16:** 836–856

Sekhon RS, Lin H, Childs KL, Hansey CN, Buell CR, de Leon N, Kaeppler SM (2011) Genome-wide atlas of transcription during maize development. Plant J **66:** 553–563

Szymanski DB, Cosgrove DJ (2009) Dynamic coordination of cytoskeletal and cell wall systems during plant cell morphogenesis. Curr Biol **19:** R800–R811

Van Damme D, Coutuer S, De Rycke R, Bouget FY, Inzé D, Geelen D (2006) Somatic cytokinesis and pollen maturation in *Arabidopsis* depend on TPLATE, which has domains similar to coat proteins. Plant Cell **18:** 3502–3518

Van Damme D, Gadeyne A, Vanstraelen M, Inzé D, Van Montagu MC, De Jaeger G, Russinova E, Geelen D (2011) Adaptin-like protein TPLATE and clathrin recruitment during plant somatic cytokinesis occurs via two distinct pathways. Proc Natl Acad Sci USA **108:** 615–620

van Zanten M, Snoek LB, Proveniers MC, Peeters AJ (2009) The many functions of ERECTA. Trends Plant Sci **14:** 214–218

Vidali L, McKenna ST, Hepler PK (2001) Actin polymerization is essential for pollen tube growth. Mol Biol Cell **12:** 2534–2545

Walker KL, Müller S, Moss D, Ehrhardt DW, Smith LG (2007) Arabidopsis TANGLED identifies the division plane throughout mitosis and cytokinesis. Curr Biol **17:** 1827–1836

Wang H, Tse YC, Law AH, Sun SS, Sun YB, Xu ZF, Hillmer S, Robinson DG, Jiang L (2010) Vacuolar sorting receptors (VSRs) and secretory carrier membrane proteins (SCAMPs) are essential for pollen tube growth. Plant J **61:** 826–838

Xu T, Wen M, Nagawa S, Fu Y, Chen JG, Wu MJ, Perrot-Rechenmann C, Friml J, Jones AM, Yang Z (2010) Cell surface- and rho GTPase-based auxin signaling controls cellular interdigitation in Arabidopsis. Cell **143:** 99–110

Yalovsky S, Bloch D, Sorek N, Kost B (2008) Regulation of membrane trafficking, cytoskeleton dynamics, and cell polarity by ROP/RAC GTPases. Plant Physiol **147:** 1527–1543

Yang Z, Lavagi I (2012) Spatial control of plasma membrane domains: ROP GTPase-based symmetry breaking. Curr Opin Plant Biol **15:** 601–607

Zhang X, Facette M, Humphries JA, Shen Z, Park Y, Sutimantanapi D, Sylvester AW, Briggs SP, Smith LG (2012) Identification of PAN2 by quantitative proteomics as a leucine-rich repeat-receptor-like kinase acting upstream of PAN1 to polarize cell division in maize. Plant Cell **24:** 4577–4589